Journal of The Electrochemical Society

The Electrochemical Society
Advancing solid state & electrochemical science & technology

OPEN ACCESS

Enhancement in the Selectivity and Sensitivity of Ni and Pd Functionalized MoS_2 Toxic Gas Sensors

To cite this article: Levna Chacko *et al* 2020 *J. Electrochem. Soc.* **167** 106506

View the article online for updates and enhancements.

This content was downloaded from IP address 202.209.187.131 on 06/07/2020 at 09:16

Journal of The Electrochemical Society, 2020 **167** 106506

Enhancement in the Selectivity and Sensitivity of Ni and Pd Functionalized MoS_2 Toxic Gas Sensors

Levna Chacko,[1] Ettore Massera,[2] and P. M. Aneesh[1,z]

[1]*Department of Physics, Central University of Kerala, Tejaswini Hills, Periye, Kasaragod, Kerala 671316, India*
[2]*ENEA Research Centre, 80055 Portici, Italy*

Atmospheric pollution is one of the major aspects of concern which led to the research of sensors for the detection of toxic gases. The supreme surface-to-volume ratio makes two-dimensional MoS_2 a promising material to be used as an electronic sensor. Here, we demonstrate the fabrication of a high-performance gas sensor based on atomic-layered MoS_2 nanoflakes synthesized by a facile hydrothermal process. Structural and morphological studies confirmed the formation of few-layered phase pure hexagonal MoS_2 nanoflakes. The results demonstrate that the Pd-MoS_2 layers exhibited a very high relative response to NO gas (700%) at 2 ppm concentration with a minimum NO detection limit of 0.1 ppm and Ni-MoS_2 demonstrated a relative response of 80% towards H_2S gas with a limit of detection of 0.3 ppm with good repeatability and selectivity, owing to the increased adsorption energy of NO on Pd-MoS_2 and H_2S on Ni-MoS_2 through the formation of $PdNO_x$ and NiS_2 complexes respectively. The improved sensing performance of this MoS_2-based sensor also suggests the great potential and possibility of MoS_2 related 2D materials and its combinations for the development of futuristic highly sensitive nanosized gas sensors suitable for anti-pollution automotive system and as volatile biomarkers.

© 2020 The Author(s). Published on behalf of The Electrochemical Society by IOP Publishing Limited. This is an open access article distributed under the terms of the Creative Commons Attribution 4.0 License (CC BY, http://creativecommons.org/licenses/by/4.0/), which permits unrestricted reuse of the work in any medium, provided the original work is properly cited. [DOI: 10.1149/1945-7111/ab992c]

Manuscript submitted March 23, 2020; revised manuscript received May 13, 2020. Published June 12, 2020. *This paper is part of the JES Focus Issue on 2D Layered Materials: From Fundamental Science to Applications.*

In the present scenario, detection and monitoring of toxic gases leading to tremendous deterioration of atmospheric environment as a result of industrial and automobile exhausts, increased population, combustion of fossil fuels, excessive use of chemicals in scientific, industrial and agricultural fields, explosives are of great demand for environmental and national security and for a sustainable biosphere. Researchers have studied on a variety of materials such as organic materials (polymers, porphyrins)[1,2] metal-oxides,[3] carbon nanotubes,[4] graphene and based-oxides[5,6] for the sensing of toxic gases such as NH_3, NO_2, NO, SO_2, CO, CO_2, organic vapors etc. NO, being one of the common and toxic air pollutants from automobile exhausts, combustion of fossil fuels, home heaters, furnace exhausts, arc welding, electroplating and power plants. On reaction with chemicals produced from sunlight, NO forms nitric acid which is a major constituent of acid rain and it also leads to the formation of ozone, smog etc. When inhaled by human beings, NO causes severe damage to human respiratory organs and nerves. Apart from this, NO is an abundant and signaling molecule produced in human body having many pathophysiological roles and is detected in the exhaled breaths of humans. The variations in the NO exhalation profile are a significant tool for understanding the normal and diseased functioning of lung and serves as a biomarker for lung diseases and pulmonary inflammations such as bronchial asthma.[7,8] Similarly, H_2S is also identified as an endogenous mediator in human body. Morselli-Labate et al.[9] demonstrated the presence of higher levels of H_2S and NO in the exhaled breaths of chronic pancreatitis.

Currently, owing to the unique physical, chemical, optical and electrical properties, two-dimensional (2D) layered nanomaterials show intriguing prospects for sensor application. Inspired by the enhanced performance of graphene and graphene-based nanomaterials for gas sensing applications because of their high sensitivity, large specific surface area, fast electron transport kinetics and strong surface activities led to increased research efforts on other graphene analogues for efficient and enhanced gas sensing. Also, the main drawbacks of metal oxide-based sensors such as the requirement of high operating temperatures, the easiness to get poisoned under sulfur atmosphere, long recovery periods, limited maximum sensitivity etc. stimulated an extensive research for highly sensitive and portable sensors that require low operating temperatures. Two-dimensional (2D) layered material, MoS_2 have aroused great research interest as a promising gas sensing material due to their high surface-to-volume ratio, high surface activities and sensitivities, fast response time and good stability.[10–13] Especially, the semiconducting nature of MoS_2 with suitable and tunable band gap energies has made it more desirable than graphene-based gas sensors.[14–17]

The direct band gap of MoS_2 is being considerably exploited and extensive theoretical and experimental research investigations are performed on the fabrication of MoS_2 nanodevices. Apart from these, the high surface-to-area ratio of 2D MoS_2 provides new avenues making MoS_2 and its various combinations as excellent sensing materials to various analytes such as NH_3, NO_2, H_2S, NO, humidity, SO_2, H_2 etc. and has been demonstrated by several research groups.[18–24] Yue et al. investigated the adsorption of a wide range of gas molecules such as H_2, O_2, H_2O, NH_3, NO, NO_2 and CO on monolayer MoS_2 using first-principles calculations. They also studied the effect of charge transfer mechanism between the adsorbed molecule and MoS_2 on the application of an external electric field.[25] In order to completely actualize the gas sensing capability of MoS_2, Zhao and co-workers demonstrated the adsorption of various gas molecules including CO, CO_2, NH_3, NO, NO_2, CH_4, H_2O, N_2, O_2 and SO_2 employing the first-principles calculations. It was found that the binding of NO, NO_2 and SO_2 with MoS_2 is the strongest among the other gas molecules.[19] In another report Li et al. fabricated MoS_2 FET devices consisting of single and multilayer MoS_2 films to detect the adsorption of NO and it was found that the multilayer films exhibited high sensitivity to NO with a detection limit of 0.8 ppm.[26] Apart from these, several research works were also performed on MoS_2-based bio and DNA sensors,[27–29] that find potential application as cancer biomarkers.[30,31]

Being a widely studied material for gas sensing applications, ZnO possess large specific surface area, high carrier mobility, non-toxicity, good electrochemical stability etc.[31] Also our earlier report on MoS_2-ZnO has already demonstrated its bio-activity presenting as an effective agent for anti-angiogenesis and anti-cancer theranostics.[32] Moreover, several reports suggest the capability of Pd and Ni to adsorb certain molecules and form complexes leading to improved selectivity. Based on first principle calculations Wei et al.[33] have reported the interaction of H_2S and SO_2 molecule with Ni-MoS_2 surface by strong adsorption energy and has been proposed as a novel gas adsorbent to be used in SF_6-insulated equipment. Reports also suggests the ability of Pd to form complexes such as the

[z]E-mail: aneeshpm@cukerala.ac.in

hydrogen sensing performance of Pd functionalised MoS_2 by forming change in the work function of Pd upon transforming to PdH_x.[34] In this study, different MoS_2-based such as pure MoS_2, MoS_2-ZnO, MoS_2-Ni and MoS_2-Pd sensor devices were fabricated. The gas sensing characteristics and mechanisms of these sensors on exposure to NO, NO_2, NH_3 and H_2S gases were analyzed and their selectivity, sensitivity and repeatability were assessed. The enhanced response of Pd-MoS_2 and Ni-MoS_2 sensors towards NO and H_2S gases respectively can be exploited for application as both automobile pollution control system and as volatile biomarkers.

Experimental

MoS_2 nanoflakes were synthesized by simple hydrothermal method as mentioned in our earlier report[35] using sodium molybdate dihydrate ($Na_2MoO_4{\cdot}2H_2O$) and thiourea (CH_4N_2S) as precursor materials at a growth temperature of 200 °C for 12 h. Exfoliated flakes of MoS_2 for the device fabrication were obtained by sonicating a 2 mg ml^{-1} solution of the as-synthesized MoS_2 powder in iso-propanol for 3 h. Stochiometric amounts of nickel acetate dehydrate ($Ni(CH_3COOH).H_2O$), dichlorobis(triphenylphosphine) palladium(II), and ZnO nanoparticles were added into MoS_2 to obtain MoS_2-Ni, MoS_2-Pd and MoS_2-ZnO nanostructures.

The architecture of the fabricated sensor is depicted in Fig. 1. Sensing devices were fabricated on a single side polished n-type, ⟨1 0 0⟩ orientation, (1–100) Ωcm resistivity silicon wafer. The wafer was cleaned by RCA (Radio Corporation of America) method to remove the organic contaminants, native oxides and metallic contaminants. 1 μm SiO_2 layer was grown on Si wafer using thermal oxidation method. This was coated with AZ5214E image reversal positive photoresist and the patterning was carried out using MJB4 optical lithography unit. Patterns were developed in MF26A solution. Sensing electrodes, 20 nm chromium and 100 nm gold, were deposited by sputtering technique. Finally, the wafer was subjected to lift-off in acetone, cleaning by IPA and drying under N_2 to get the patterned device structure. A few-layer MoS_2 flakes for the active channel were exfoliated using a conventional ultrasonication method and then transferred them onto a SiO_2/Si substrate by drop-casting. The gas response of different MoS_2-based sensors was measured using two-probe measurement system in synthetic air environment. The sensing performance of the sensors with and without exposure to various toxic gases such as NH_3, H_2S, NO and NO_2 were measured at room temperature with a bias voltage of 1 V.

X-ray diffraction (XRD) characterization with Cu $K\alpha_1$ radiation ($\lambda = 1.5406$ Å) using Rigaku MiniFlex 600 diffractometer was employed to analyze the crystalline structure and phase purity of nanostructured MoS_2 samples. Horiba JOBIN YVON LabRAM HR Raman Spectrometer equipped with 514.5 nm Ar-ion laser as the excitation source was used for Raman studies. Field emission scanning electron microscopy (FE-SEM ΣIGMA, ZIESS) was used in order to investigate the surface morphology of nanostructured MoS_2. The current–voltage (I-V) characteristics of the device were measured using Agilent Technologies B1500A semiconductor device analyser. A two-electrode configuration was employed for the sensing measurements. The sensitivity of the sensor was monitored by applying a constant bias voltage of 1 V on the sensor and recording the variation in the current using Keithley 237 high voltage source measure unit. Prior to the measurements, the gas chamber was purged with synthetic gas. After a constant current was observed, the sensor was exposed to various analytes.

Results and Discussion

The crystalline structure, phase, purity and morphology of the MoS_2 nanostructure were investigated through X-ray diffraction (XRD), Raman analysis and field emission scanning electron microscopic (FESEM) images. The XRD pattern of MoS_2, MoS_2-Pd, MoS_2-Ni and MoS_2-ZnO nanostructures synthesized by hydrothermal method is shown in Fig. 2a. It is obvious that that all the diffraction peaks of MoS_2 and MoS_2-Ni can be indexed to hexagonal phase of crystalline MoS_2 without the presence of any secondary phases. The diffractograms of MoS_2-ZnO and MoS_2-Pd consists of planes corresponding to ZnO and Pd in addition to MoS_2 peaks. The distinct peak at (0 0 2) orientation of MoS_2 represents the well-ordered stacking of S-Mo-S layers.[36,37] The calculated grain size and lattice parameters of the nanostructures are represented in Table I. The Raman shift between the two characteristic peaks, E^1_{2g} and A_{1g}, representing in–plane and out–of–plane vibration modes respectively, indicates the presence of few-layer MoS_2 and is shown in Fig. 2b.[38,39] The in–plane E^1_{2g} mode originates from opposite vibration of two S atoms with respect to the Mo atom while the A_{1g} mode represents the out–of–plane vibration of only S atoms in opposite directions.[40] Also, in a report, Agrawal et al.[41] have reported that the terrace sites favor the formation of E^1_{2g} mode, whereas A_{1g} mode is preferred by the edges of MoS_2 and the increase in the intensity of A_{1g} mode represents the increased density of the edge-enriched MoS_2 flakes. The frequency difference between E^1_{2g} and A_{1g} peaks can be attributed to the mixed signal from different layered structure of MoS_2 nanoflakes.[41] Thus, the observed frequency shift in MoS_2-ZnO, MoS_2-Ni and MoS_2-Pd Raman peaks

Table I. Grain size and lattice parameters of MoS_2, MoS_2-ZnO, MoS_2-Ni and MoS_2-Pd nanostructures synthesized by hydrothermal method.

		Lattice Parameters (Å)	
Sample	Grain Size (nm)	a	c
MoS_2	5	3.12	12.63
MoS_2-ZnO	6	3.12	12.74
MoS_2-Ni	6	3.12	12.84
MoS_2-Pd	6	3.12	12.70

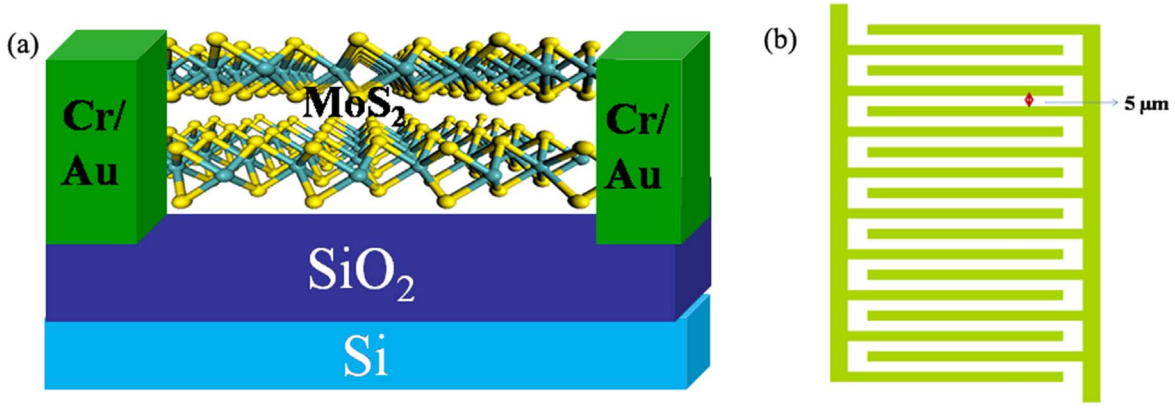

Figure 1. (a) Architecture of MoS_2-based sensing device, (b) Pattern of Cr/Au electrodes used in the sensor device.

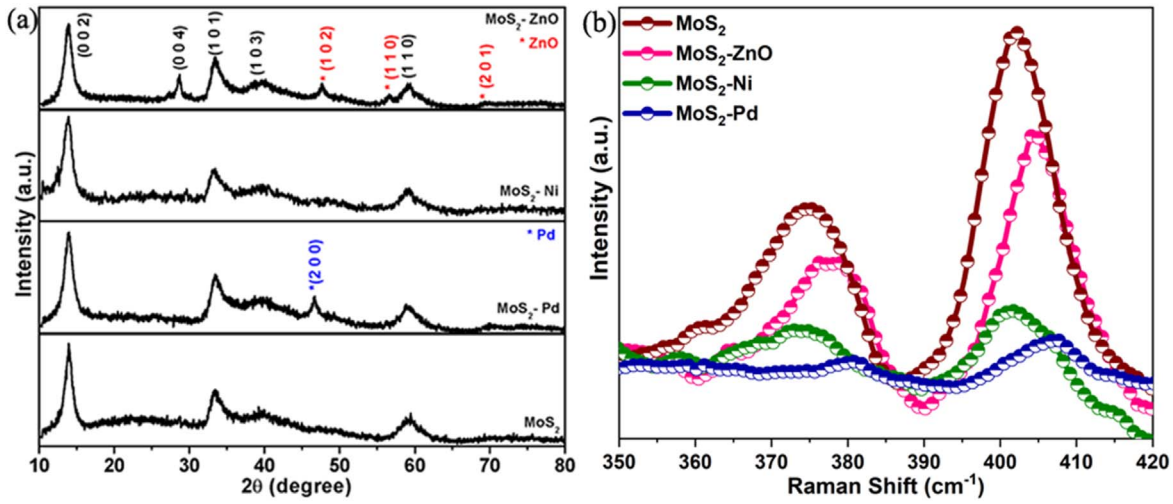

Figure 2. (a) XRD pattern and (b) Raman spectra of MoS_2, MoS_2-Pd, MoS_2-Ni and MoS_2-ZnO nanostructures.

can be ascribed to some structural changes and long-range Coulomb interaction in addition to the van der Waals interlayer coupling during functionalization.[42]

The morphology of the as-prepared MoS_2, MoS_2-ZnO, MoS_2-Ni and MoS_2-Pd nanostructures were identified from FESEM (Fig. 3) showing uniform curly–like structure assembled into the nanoflakes, indicating that the samples have large specific surface areas. Presence of ZnO nanoparticles is also visible along with MoS_2 nanoflakes in the MoS_2-ZnO morphology (Fig. 3c), whereas, closely aggregated nanoflakes like structures are observed in the MoS_2-Pd morphology (Fig. 3d).

Energy dispersive X-ray (EDS) measurement of the samples was performed to identify the chemical composition and is shown in Fig. 4. Presence of Ni, Zn, O and Pd were observed supporting the formation of MoS_2-Ni, MoS_2-ZnO and MoS_2-Pd nanosystems.

In order to identify the suitability of MoS_2 and other nanostructures for the sensing applications, the I-V characteristic of the device without the presence of sensing gas was studied by two probe method and is shown in Fig. 5. The linear characteristics of the I-V curve confirm the ohmic nature of the contact with a resistance of the order of 176 Ω, 202 Ω, 210 Ω and 227 Ω for MoS_2, Ni- MoS_2, Pd-MoS_2 and MoS_2- ZnO nanostructures. Compared to other systems,

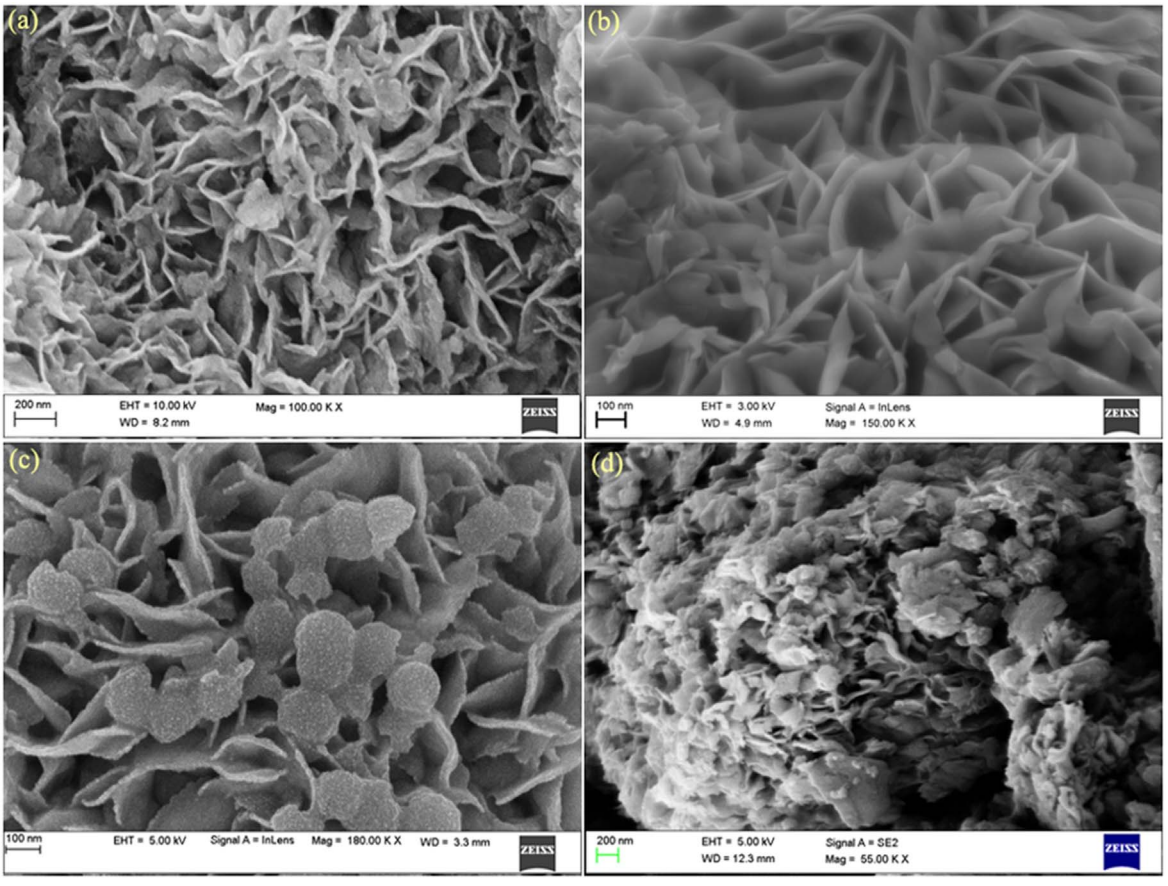

Figure 3. FESEM images of (a) MoS_2 (b) Ni-MoS_2 (c) MoS_2-ZnO and (d) Pd-MoS_2 nanostructures.

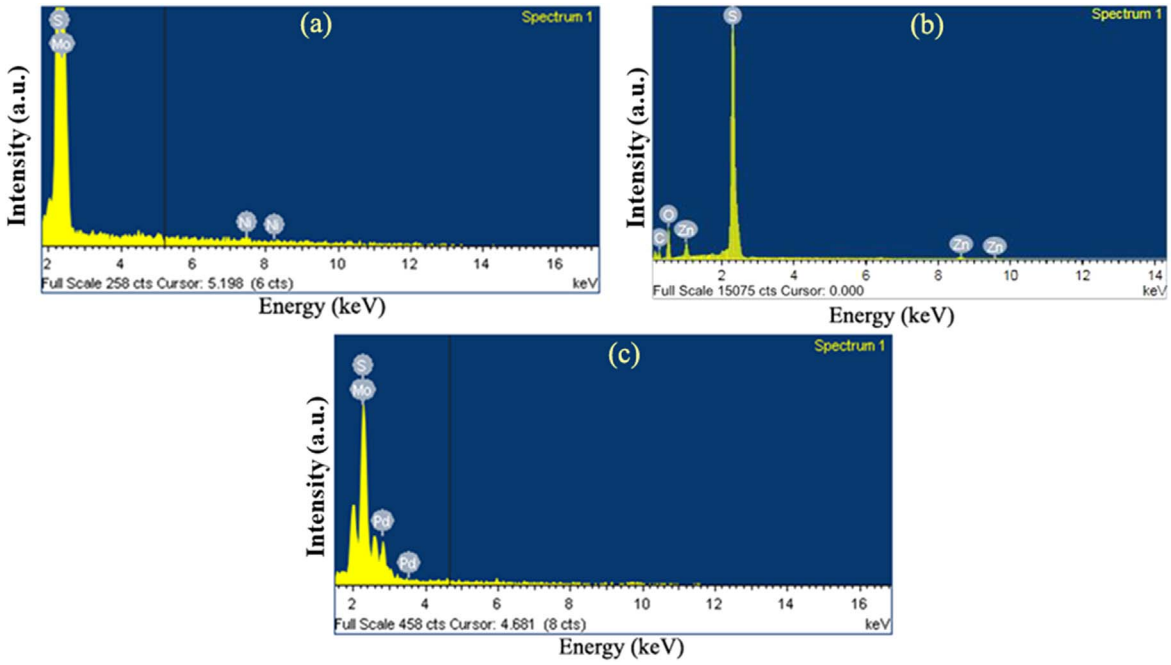

Figure 4. EDS spectra of (a) Ni-MoS_2 (b) MoS_2-ZnO and (c) Pd-MoS_2 nanostructures.

Pd-MoS_2 nanostructures are exhibiting a small forward current under light illumination (resistance of 198 Ω) representing the photoresponsive nature due to formation of more electron-hole pairs upon light illumination.

Gas sensing properties of pure MoS_2, Ni and Pd functionalized MoS_2 and MoS_2-ZnO nanocomposite sensor upon exposure to various gases were investigated using two-probe measurement system at room temperature with a bias voltage of 1 V. Fig. 6a illustrates the dynamic sensing response of MoS_2 sensor against various reducing (NO, H_2S, NH_3) and oxidizing (NO_2) gases at 2 ppm concentration. The relative response of the sensor was defined as

$$S = \frac{\Delta I}{I} = \frac{I_g - I_0}{I_o} \times 100 \quad [1]$$

where I_g is the current during the gas exposure, and I_0 is the current in the dry air. When the MoS_2 sensor is exposed to the gases, a charge transfer between the gaseous species and MoS_2 nanoflakes occurs resulting in a change in their carrier concentration/ conductance, which serves as an important principle for the working of sensing devices.

On exposure to synthetic air, oxygen molecules get adsorbed to the surface of MoS_2 nanoflakes and form surface acceptor states O_2^- (ads), O^- (ads), O^{2-} (ads) that captures free electrons from the conduction band of the MoS_2 and lead to formation of an electron depletion layer near the surface of n-type MoS_2. At low temperature, oxygen is adsorbed in its molecular state O_2^-, whereas at high temperature it dissociates as atomic O^- and O^{2-}.[43,44]

$$O_2(g) + e^- = O_2^-(ads) \quad T < 100\ ^\circ C \quad [2]$$

$$O_2^-(ads) + e^- = 2\ O^-(ads) \quad 100\ ^\circ C < T < 300\ ^\circ C \quad [3]$$

$$O^-(ads) + e^- = O^{2-}(ads) \quad T > 300\ ^\circ C \quad [4]$$

Oxygen molecules are electron acceptors, which accept electrons from MoS_2 and result in the decrease of electrons concentration leading to decrease in the conductance of the sensor. On exposure to oxidizing gases, these gas molecules react with MoS_2 with an

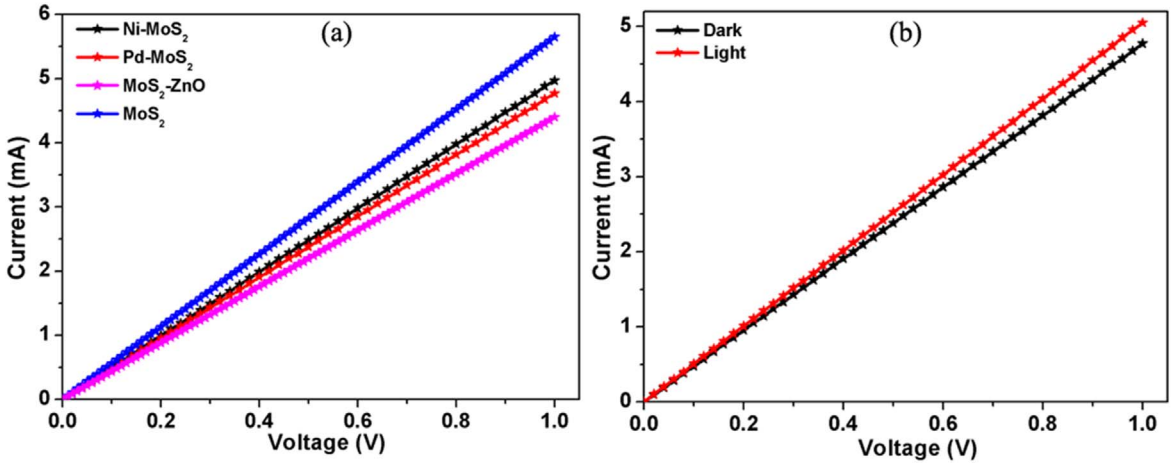

Figure 5. I-V characteristics of (a) MoS_2, Ni-MoS_2, Pd-MoS_2 and MoS_2-ZnO nanostructures under dark condition and (b) Pd- MoS_2 nanostructures under dark and light illumination condition.

increased quantity of oxygen ions due to further oxidation leading to a decrease in the sensor conductance. Whereas, on exposure to reducing gases, the gas molecules release the trapped electrons back to the conduction of MoS_2 leading to an increase in the electron concentration and conductance. That is the sensor conductance is found to decrease on exposure to oxidizing gases, whereas it increased for reducing gases indicating p-type and n-type conduction in nanocrystalline MoS_2 sensor respectively. For example, when the sensor is exposed to oxidizing gas NO_2, being an electron acceptor due to an unpaired electron from nitrogen atom, NO_2 results in p-type doping and hence they shift the Fermi-level of MoS_2 towards valence band edge. NO_2 gets adsorbed onto MoS_2 surface and the strong adsorption of NO_2 dominates over O_2^- and creates an extended depletion layer as NO_2 serves as electron acceptor which tends to the withdrawal of electrons from the conduction band of the sensing material MoS_2. As a result, the electron concentration in the conduction band of MoS_2 is found to decrease, thus increasing the resistance of MoS_2 sensor. This resulted in a decrease in sensor conductivity upon exposure to oxidizing gases.[45,46] As observed in Fig. 6a it is evident that pure MoS_2 have a dynamic response towards various gases with a poor cross selectivity. But MoS_2 based sensors can be used for identifying ammonia leakage from ammonia refrigerants used in large industries. Automobile exhaust gases include toxic NO_x, SO_2, CO etc. and these MoS_2 sensors can be used to detect the average increase or decreased dosage of automobile exhaust.

In contrast to the general sensing mechanism, the sensor conductance of our MoS_2 sensor is found to decrease for reducing gases, which usually serves as electron donors in the charge transfer process. Usually, the reducing gases donate electrons to the conduction band of MoS_2 thus increasing the carrier concentration in MoS_2 and hence shift the Fermi-level of MoS_2 towards conduction band edge.[46,47] There are several factors that affect the electrical conductance of the sensor such as the chemisorbed oxygen, defects such as vacancies, interstitial sites, chemical potential etc.

Fan et al.[48] reported a reversal in the conductance during ZnO nanowire based NH_3 sensing. They observed that at room temperature the Fermi level of the material lies above the chemical potential of ammonia gas. As electrons transfer from the material with higher chemical potential to one with lower chemical potential until the system reaches equilibrium, ammonia withdraws electrons from ZnO nanowire leading to a decrease in the conductance. Whereas, at elevated temperature, they observed a downshift in the Fermi energy level of nanowire with a decrease in the chemical potential of NH_3. Similarly, the decrease conductance observed on exposure of reducing gases at room temperature can also be attributed to the higher chemical potential of MoS_2 compared to that of gases. In addition, the effect of oxygen molecules and the reaction of these reducing gases to form oxygen species also contribute to the enhanced electron withdrawing from MoS_2. As a consequence of which the reducing gases are expected to induce a p-doping effect on MoS_2.

The p-doping effect created by exposure of MoS_2 sensor to NO leading to a decrease in current has been demonstrated by Li and co-authors with a detection limit of 0.8 ppm.[26] Barazzouk et al.[49] reported the influence of chemisorbed oxygen species in the sensing mechanism with an increase in resistance of MoO_3 towards both NO and NO_2 gases. The observance of decreasing electrical conductance on exposure to both oxidizing and reducing gases in MoS_2 can be ascribed to these factors discussed above.

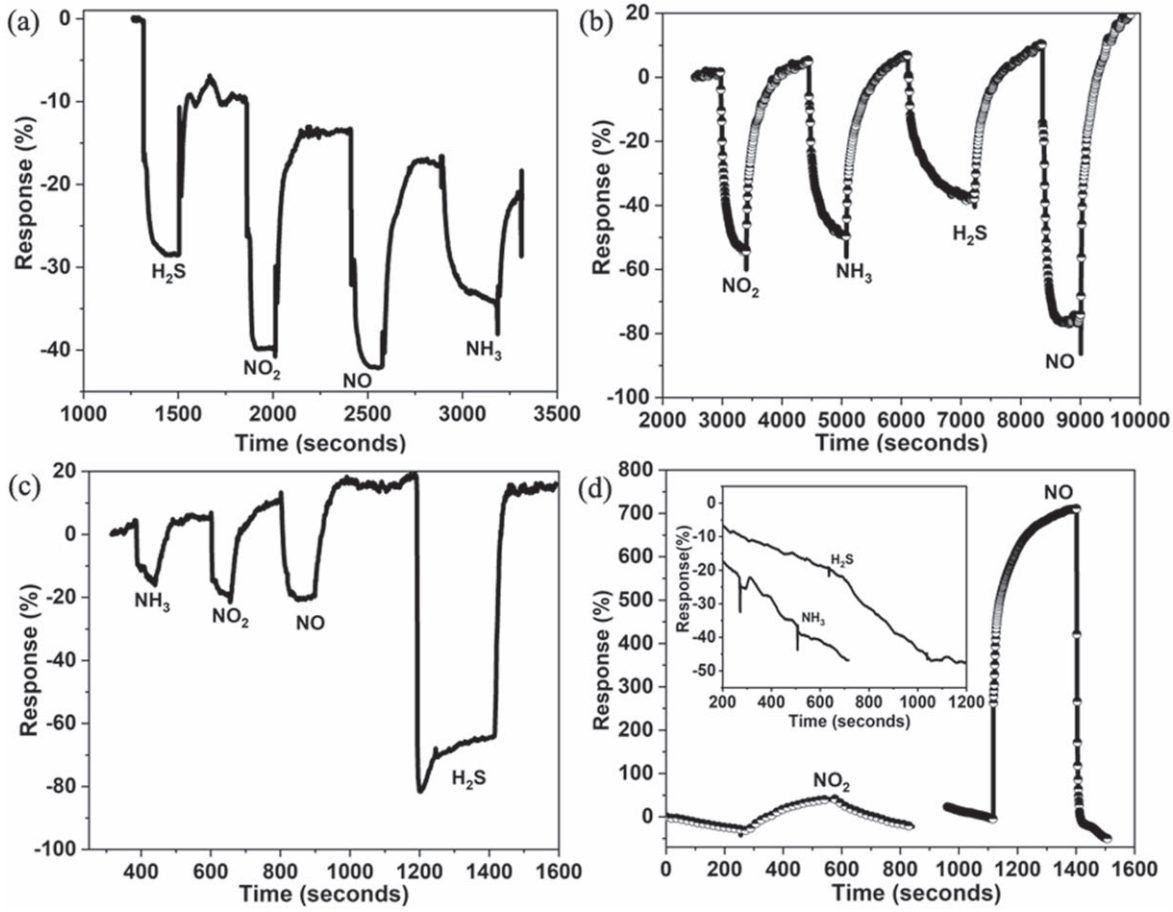

Figure 6. Current change of (a) MoS_2, (b) MoS_2-ZnO, (c) MoS_2-Ni and (d) MoS_2-Pd gas sensors upon exposure to 2 ppm concentration of NH_3, H_2S, NO_2 and NO gases.

In order to stabilize and enhance the cross sensitivity of MoS_2 based sensors, we functionalized MoS_2 using ZnO, Ni and Pd. The results shows that after the incorporation of ZnO, Ni and Pd, the cross-sensitivity has improved for MoS_2-ZnO, MoS_2-Ni and MoS_2-Pd and is shown in Figs. 6b–6d. MoS_2-ZnO displays a slightly increased sensitivity towards NO, whereas MoS_2-Ni sensor shows excellent selectivity towards H_2S gas and Pd functionalized MoS_2 exhibited a remarkable increase in the response towards NO gas. The MoS_2-Pd sensor does not exhibit any response towards H_2S and NH_3. These results can be attributed to the strongest interaction and charge transfer between the respective gases and active sensing material MoS_2, large adsorption and binding energies and also to the changes in the bond lengths. In case of Ni-MoS_2 sensor, a higher response is observed towards H_2S gas with sensitivity of around 80%. The incorporation of Ni into the MoS_2 matrix can lead to the formation of NiS_2 phases on exposure to H_2S gas. The increase in the adsorption energy of H_2S towards Ni-MoS_2 enhanced the charge transfer compared to other reactive gases showing low adsorption energies towards Ni-MoS_2.[50]

Pd is a metal with high work function (5.1–5.6 eV) compared to MoS_2 (4.3–5.2 eV). As a result, electrons are transferred from MoS_2 to Pd creating a p-doping effect of Pd on MoS_2. On exposure to NO and NO_2, Pd forms $PdNO_x$ complexes, with a work function lower than that of both Pd and MoS_2. Thus, the electron transferred from MoS_2 will be compensated by the transfer of electron from the $PdNO_x$ complexes to MoS_2 and that results in the increase of the sensing current on the exposure of NO and NO_2. The theoretical study on the adsorptions of NO, NO_2, CO, SO_2 and NH_3 on MoS_2 nanotube represents the higher adsorption energy of NO (E_{ads} = 129.3 meV) on MoS_2 nanotube compared to that on monolayer MoS_2 (E_{ads} = 77.4 meV). An increased charge transfer was also observed between NO and MoS_2 nanotube (0.029 e) compared to monolayer MoS_2 (0.005 e).[51] Hence, we can say that the increased cross-sensitivity of Pd-MoS_2 towards NO is due to the higher adsorption energy of NO on MoS_2-Pd nanoflakes and associated charge transfer between Pd-MoS_2 and NO gas.

In a report, Niu et al. demonstrated the gas sensing behavior of N and Si co-doped graphene nanosheets with response value of about 26 ± 1% at 21 ppm of NO_2 concentration.[52] Cho and co-authors obtained a sensitivity of about ~26% for NO_2 at concentration of 20 ppm and room temperature for CVD synthesized layered MoS_2.[46] In this study, we obtained a high relative response of about 80% for MoS_2-ZnO and 700% for MoS_2-Pd gas sensor at 2 ppm NO concentration and a relative response of 80% towards 2 ppm H_2S for MoS_2-Ni, which is significantly higher compared to other MoS_2 and graphene based sensors[17,53–55] due to increased charge transfer between the analyte and MoS_2. The sensing mechanism in MoS_2 based sensors on exposure to air and other reactive gases are pictured in Fig. 7.

The responses of MoS_2-Ni and MoS_2-Pd based sensors to different concentrations of H_2S and NO respectively are shown in Figs. 8a and 8b respectively. As the concentration of gas molecules increases, more surface dipoles are formed, which results in more electron transfer between MoS_2 and analyte, thus increasing their interaction leading to higher response.[56] The response increases rapidly with increasing concentration of H_2S in the range of 0.3–2 ppm indicating good sensitivity of MoS_2-Ni sensor towards different H_2S concentrations. Similarly, response of MoS_2-Pd sensor upon exposure to NO with concentrations ranging from 0.1 to 2 ppm indicating the good sensitivity of MoS_2-Pd sensor towards NO gas. From the slope of sensor response vs target gas concentration plot (inset of Figs. 8a and 8b) we got the sensitivity of MoS_2-Ni and MoS_2-Pd sensors as 36 and 227%/ppm respectively. The repeatability of MoS_2-Ni towards H_2S over seven periodic sensing cycles and that of MoS_2-Pd sensor towards NO over six periodic sensing cycles are shown in Figs. 8c and 8d respectively. It was found that

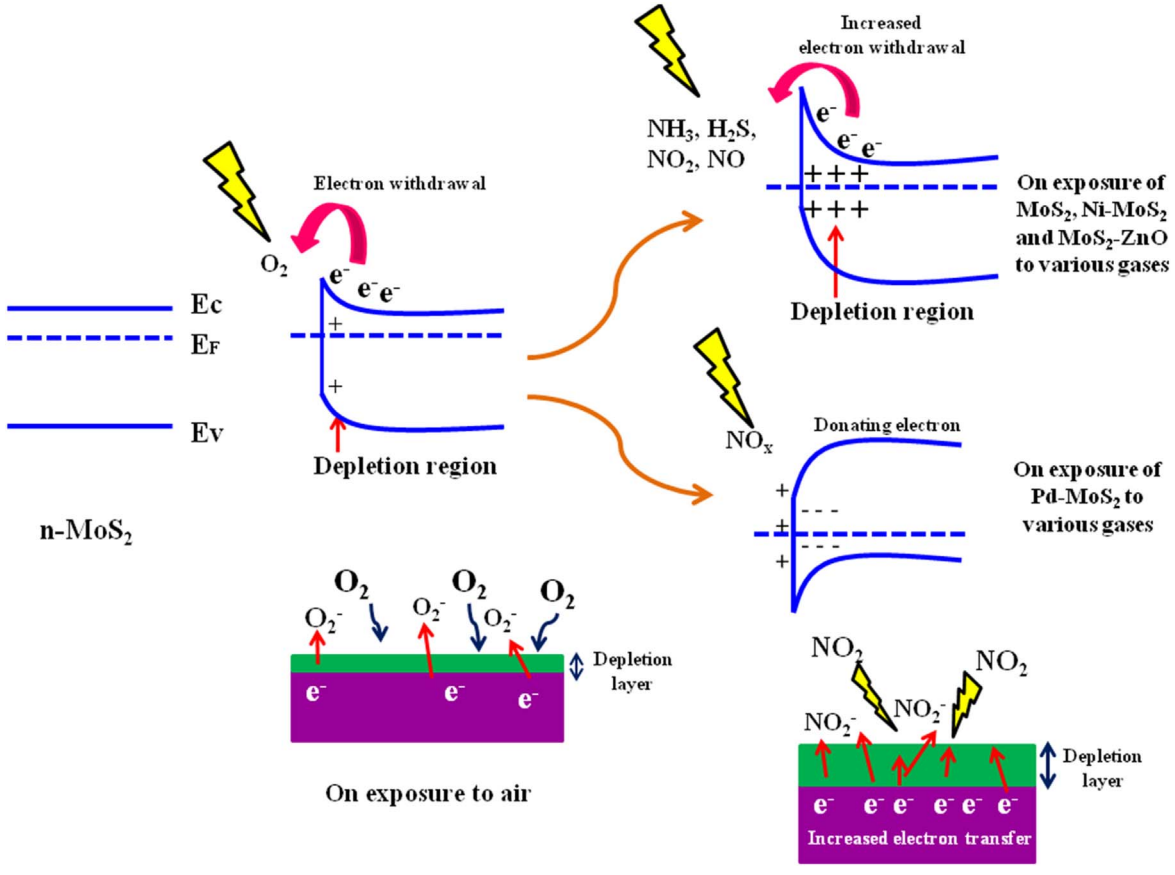

Figure 7. Schematic illustration of proposed band edge alignment across MoS_2 and Ni, ZnO, Pd functionalized MoS_2 on exposure towards various gases.

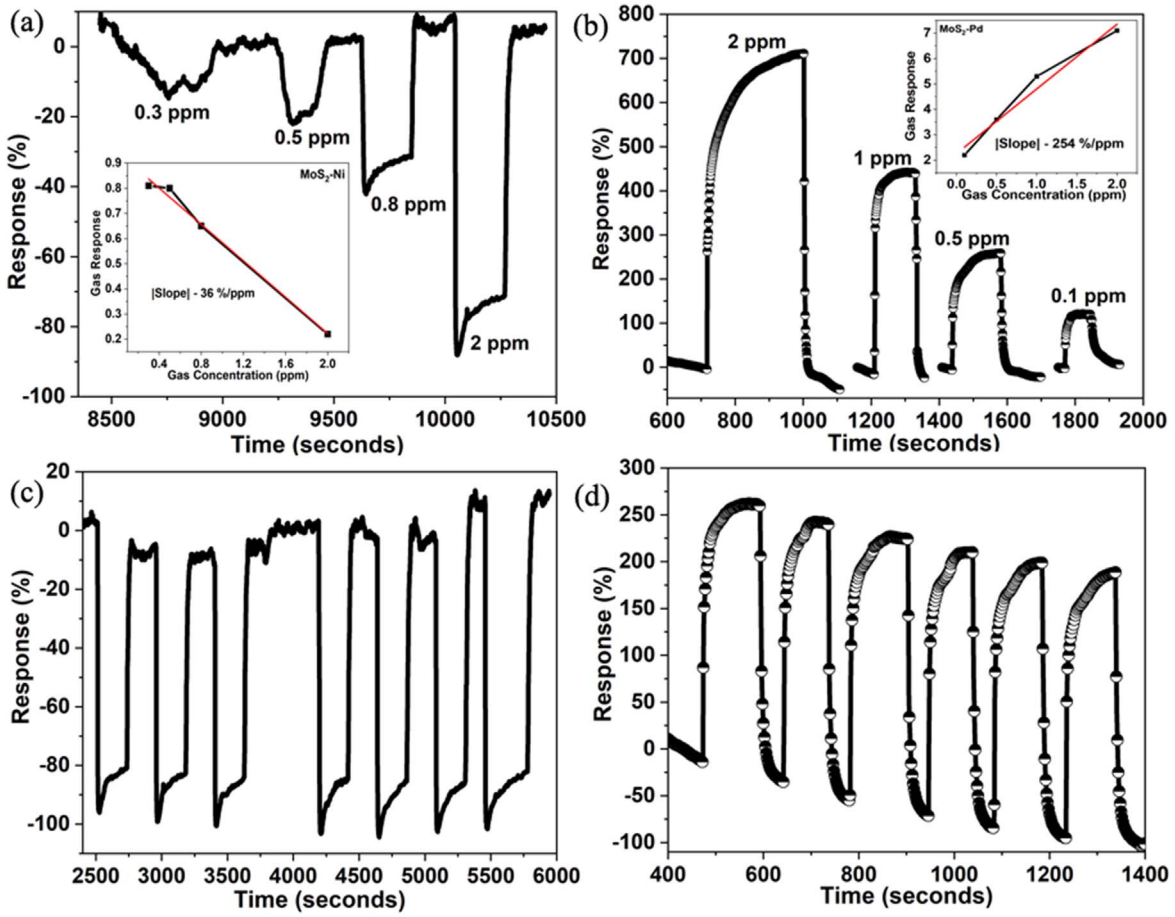

Figure 8. Response variation of (a) MoS_2-Ni based sensor as a function of H_2S concentrations with inset showing the slope of sensor response vs target gas concentration of MoS_2-Ni sensor (b) MoS_2-Pd based sensor as a function of NO concentrations with inset showing the slope of sensor response vs target gas concentration of MoS_2-Pd sensor, Repeatability of (c) MoS_2-Ni gas sensor upon exposure to successive pulses of 2 ppm H_2S gas and (d) MoS_2-Pd gas sensor upon exposure to successive pulses of 0.5 ppm NO gas.

sensors exhibit almost stable response upon repeated exposure to H_2S and NO confirming the excellent repeatability of the sensor material suitable for automotive antipollution system. The results also suggest that MoS_2-Pd sensor having high response towards NO is a promising biomarker for pulmonary inflammations and a combination of both MoS_2-Pd and MoS_2-Ni sensors can serve as a biomarker for chronic pancreatitis. It can be stated that the presence of high surface area makes MoS_2 nanoflakes highly sensitive to the adsorption of gaseous molecules on the surface causing high sensitivities.

The humidity effect on MoS_2 and its related systems is well recognized (Fig. 9) and it is a concern for the MoS_2 based sensor. It is observed that, on changing humidity from 5% to 55%, a current variation of 0.006 μA is noticed on MoS_2-Ni device while on MoS_2-Pd device the current variation is 1.5 μA. This humidity variations can be considered to be negligible compared to H_2S and NO gas responses on the device. It is also observed that MoS_2-Ni sensor is showing high response towards H_2S gas with a current variation of around 14 μA (response of 80%) at a concentration of 2 ppm. Whereas, the same MoS_2-Ni sensor shows small current variation of around 2–4 μA (response of 15%–20%) towards other gases (NO, NO_2, NH_3) at a concentration of 2 ppm. Similarly, in the case of MoS_2-Pd sensor, the sensor exhibits remarkable response towards NO gas at a concentration of 2 ppm with a very large current variation around 34 μA (response of 700%). On the other hand, it is evident that MoS_2-Pd sensor is showing vary small current variation of around 4 μA (response of 44%) on passing NO_2 gas at a concentration of 2 ppm. From these current variations, we confirmed the selectivity of MoS_2-Ni towards H_2S and MoS_2-Pd towards NO gas and the negligible variation in humidity compared to gas sensing.

The highly selective, sensitive and stable gas-sensing performance achieved in 2D-MoS_2 based nanostructures promises a new avenue of metal dichalcogenides toward the development of electronic sensors. However, the humidity effect should also be tested directly by measuring the gas sensing behavior while changing the humidity level and the selectivity should be discussed with the sensing results based on mixed gases, not a single gas for the complete study on the sensing characteristics of a sensor.

In conclusion, we successfully fabricated MoS_2, MoS_2-ZnO, MoS_2-Ni and MoS_2-Pd nanostructures-based sensors. The gas-sensing performance of the as-prepared MoS_2 nanostructures-based sensor was investigated towards various hazardous gases. The MoS_2-based sensors showed excellent sensing performances with high sensitivity at room temperature, which can serve as an excellent alternative to the common semiconductor metal oxide gas sensors that require high optimal working temperatures for good response. It was identified that Ni-MoS_2 sensors have high sensitivity towards detection of H_2S gas. The Pd-MoS_2 sensor exhibited excellent sensitivity, stability and high selectivity for NO detection making it an attractive candidate for automobile exhaust gas sensing applications and a promising biomarker for pulmonary inflammations. The enhanced gas sensing properties were probably attributed to the synergetic effect of MoS_2 nanoflakes with good specific

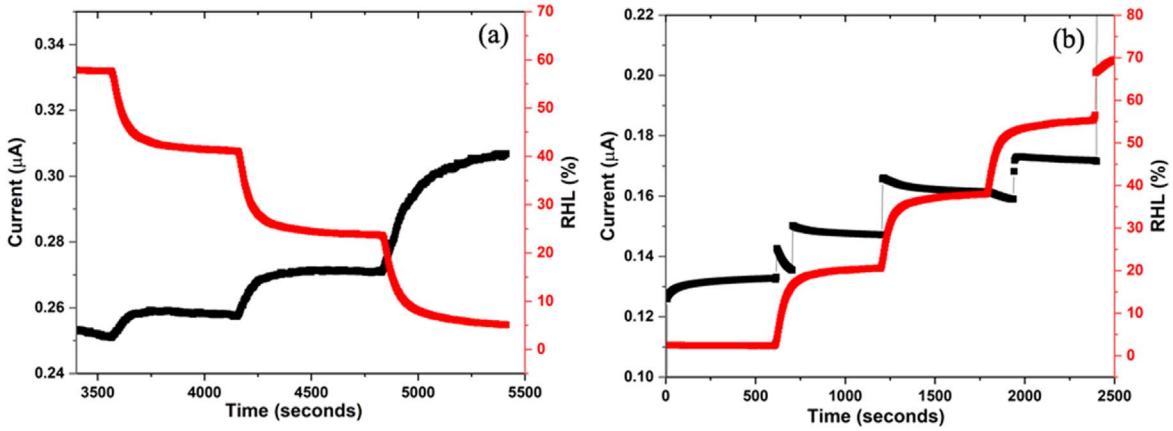

Figure 9. Humidity sensing response of (a) MoS_2-Ni and (b) MoS_2-Pd based sensor.

surface area. The results demonstrate that the MoS_2-based sensors can open up new horizons in the development of futuristic multi-functional chemical and bio-sensors.

Acknowledgments

Levna Chacko acknowledge Department of Science and Technology (DST), New Delhi, India for INSPIRE fellowship. The authors acknowledge Prof. M. K. Jayaraj, CUSAT, Kerala, India for Raman facilities under Nanoscience and Technology Initiative, DST, Government of India. The authors gratefully acknowledge Centre for Nanoscience and Engineering (CeNSE), Indian Institute of Science, Bangalore through the Indian Nano User Programme (INUP), funded by the Department of Electronics and Information Technology (DeitY), Govt. of India for device fabrication facilities.

ORCID

P. M. Aneesh https://orcid.org/0000-0002-0225-1714

References

1. Z. Jin, Y. Su, and Y. Duan, "Development of a polyaniline-based optical ammonia sensor." *Sensors Actuators, B Chem.*, **72**, 75 (2001).
2. M. Evyapan and A. D. F. Dunbar, "Applied surface science controlling surface adsorption to enhance the selectivity of porphyrin based gas sensors." *Appl. Surf. Sci.*, **362**, 191 (2016).
3. G. F. Fine, L. M. Cavanagh, A. Afonja, and R. Binions, "Metal oxide semi-conductor gas sensors in environmental monitoring." *Sensors*, **10**, 5469 (2010).
4. T. Zhang, S. Mubeen, N. V. Myung, and A. D. Marc, "Recent progress in carbon nanotube-based gas sensors." *Nanotechnology*, **19**, 332001 (2008).
5. S. S. Varghese, S. Lonkar, K. K. Singh, S. Swaminathan, and A. Abdala, "Recent advances in graphene based gas sensors." *Sensors Actuators, B Chem.*, **218**, 160 (2015).
6. S. Prezioso, F. Perrozzi, L. Giancaterini, C. Cantalini, E. Treossi, V. Palermo, M. Nardone, S. Santucci, and L. Ottaviano, "Graphene oxide as a practical solution to high sensitivity gas sensing." *J. Phys. Chem. C*, **117**, 10683 (2013).
7. P. J. Barnes and S. A. Kharitonov, "Exhaled nitric oxide : a new lung function test." *Thorax*, **51**, 233 (1996).
8. N. M. Tsoukias, Z. Tannous, A. F. Wilson, and S. C. George, "Single-exhalation profiles of NO and CO_2 in humans: effect of dynamically changing flow rate." *J. Appl. Physiol.*, **85**, 642 (1998).
9. A. M. Morselli-labate, L. Fantini, and R. Pezzilli, "Hydrogen sulfide, nitric oxide and a molecular mass 66 u substance in the exhaled breath of chronic pancreatitis patients." *Pancreatology*, **7**, 497 (2007).
10. S. Varghese, S. Varghese, S. Swaminathan, K. Singh, and V. Mittal, "Two-dimensional materials for sensing: graphene and beyond." *Electronics*, **4**, 651 (2015).
11. B. Cho et al., "Charge-transfer-based gas sensing using atomic-layer MoS_2." *Sci. Rep.*, **5**, 8052 (2015).
12. M. Donarelli, S. Prezioso, F. Perrozzi, F. Bisti, M. Nardone, L. Giancaterini, C. Cantalini, and L. Ottaviano, "Response to NO_2 and other gases of resistive chemically exfoliated MoS2-based gas sensors." *Sensors Actuators B Chem.*, **207**, 602 (2015).
13. A. Shokri and N. Salami, "Gas sensor based on MoS_2 monolayer." *Sensors Actuators B Chem.*, **236**, 378 (2016).
14. Y. Han et al., "Design of hetero-nanostructures on MoS_2 nanosheets to boost NO_2 room-temperature sensing." *ACS Appl. Mater. Interfaces*, **10**, 22640 (2018).
15. K. Kalantar-Zadeh and J. Z. Ou, "Biosensors based on two-dimensional MoS_2." *ACS Sens.*, **1**, 5 (2016).
16. S. Yang, C. Jiang, and S. Wei, "Gas sensing in 2D materials." *Appl. Phys. Rev.*, **4**, 021304 (2017).
17. H. Long, A. Harley-Trochimczyk, T. Pham, Z. Tang, T. Shi, A. Zettl, C. Carraro, M. A. Worsley, and R. Maboudian, "High surface area MoS_2/graphene hybrid aerogel for ultrasensitive NO_2 detection." *Adv. Funct. Mater.*, **26**, 5158 (2016).
18. D. Ma, W. Ju, T. Li, X. Zhang, C. He, B. Ma, Z. Lu, and Z. Yang, "The adsorption of CO and NO on the MoS_2 monolayer doped with Au, Pt, Pd, or Ni : a first-principles study." *Appl. Surf. Sci.*, **383**, 98 (2016).
19. S. Zhao, J. Xue, and W. Kang, "Gas adsorption on MoS_2 monolayer from first-principles calculations." *Chem. Phys. Lett.*, **595–596**, 35 (2014).
20. L. Yu, F. Guo, S. Liu, J. Qi, M. Yin, B. Yang, Z. Liu, and X. H. Fan, "Hierarchical 3D flower-like MoS_2 spheres : post-thermal treatment in vacuum and their NO_2 sensing properties." *Mater. Lett.*, **183**, 122 (2016).
21. A. V. Agrawal, R. Kumar, S. Venkatesan, A. Zakhidov, G. Yang, J. Bao, M. Kumar, and M. Kumar, "Photo-activated mixed in-plane and edge-enriched p-type MoS_2 flakes based NO_2 sensor working at Room temperature." *ACS Sens.*, **3**, 998 (2018).
22. D. Zhang, J. Wu, P. Li, and Y. Cao, "Room-temperature SO_2 gas sensing properties based on metal-doped MoS_2 nanoflower: an experimental and density functional theory Investigation." *J. Mater. Chem. A*, **5**, 20666 (2017).
23. S. Y. Park et al., "Highly selective and sensitive chemoresistive humidity sensors based on rGO/MoS_2 van der waals composites." *J. Mater. Chem. A*, **6**, 5016 (2018).
24. A. V. Agrawal, R. Kumar, G. Yang, J. Bao, M. Kumar, and M. Kumar, "Enhanced adsorption sites in monolayer MoS_2 pyramid structures for highly sensitive and fast hydrogen sensor." *Int. J. Hydrogen Energy*, **45**, 9268 (2020).
25. Qu Yue, Zhengzheng Shao, Shengli Chang, and Jingbo Li, "Adsorption of gas molecules on monolayer MoS2 and effect of applied electric field." *Nanoscale Research Letters*, **8**, 425 (2013).
26. H. Li, Z. Yin, Q. He, H. Li, X. Huang, G. Lu, D. W. H. Fam, A. I. Y. Tok, Q. Zhang, and H. Zhang, "Fabrication of single- and multilayer MoS_2 film- based field-effect transistors for sensing NO at room temperature." *Small*, **8**, 63 (2012).
27. T. Wang, H. Zhu, J. Zhuo, Z. Zhu, G. V. Lubarsky, J. Lin, and M. Li, "A biosensor based on ultrasmall MoS_2 nanoparticles for electrochemical detection of H_2O_2 released by cells at nM level." *Anal. Chem.*, **85**, 10289 (2013).
28. X. Wang, F. Nan, J. Zhao, T. Yang, T. Ge, and K. Jiao, "A label-free ultrasensitive electrochemical DNA sensor based on thin-layer MoS_2 nanosheets with high electrochemical activity." *Biosens. Bioelectron.*, **64**, 386 (2015).
29. X. Wang, W. Deng, L. Shen, M. Yan, S. Geb, and J. Yu, "A sensitive quenched electrochemiluminescent DNA sensor based on the catalytic activity of gold nanoparticles functionalized MoS_2." *New J. Chem.*, **39**, 8100 (2015).
30. H. Nam, B.-R. Oh, P. Chen, M. Chen, S. Wi, W. Wan, K. Kurabayashi, and X. Liang, "Multiple MoS_2 transistors for sensing molecule interaction kinetics." *Sci. Rep.*, **5**, 10546 (2015).
31. Y. Zhou, C. Gao, and Y. Guo, "UV assisted ultrasensitive trace NO_2 gas sensing based on few-layer MoS_2 nanosheet-ZnO nanowire heterojunctions at room temperature." *J. Mater. Chem. A*, **6**, 10286 (2018).
32. L. Chacko, A. Poyyakkara, V. B. S. Kumar, and P. M. Aneesh, "MoS_2-ZnO nanocomposites as highly functional agents for anti-angiogenic and anti-cancer theranostics." *J. Mater. Chem. B*, **6**, 3048 (2018).
33. H. Wei, Y. Gui, J. Kang, W. Wang, and C. Tang, "A DFT study on the adsorption of H_2S and SO_2 on Ni Doped MoS_2 monolayer." *Nanomaterials*, **8**, 646 (2018).
34. D. Baek and J. Kim, "Few-layered MoS_2 gas sensor functionalized by Pd for the detection of hydrogen." *Sensors Actuators B Chem.*, **250**, 686 (2017).

35. L. Chacko, A. K. Swetha, R. Anjana, M. K. Jayaraj, and P. M. Aneesh, "Wasp-waisted magnetism in hydrothermally grown MoS_2 nanoflakes." *Mater. Res. Express*, **3**, 116102 (2016).
36. Z. Wan, J. Shao, J. Yun, H. Zheng, T. Gao, M. Shen, N. Qu, and H. Zheng, "core–shell structure of hierarchical quasi-hollow MoS_2 microspheres encapsulated porous carbon as stable anode for Li-ion batteries." *Small*, **10**, 4975 (2014).
37. Y.-H. Tan, K. Yu, J.-Z. Li, H. Fu, and Z.-Q. Zhu, "MoS_2@ZnO nano-heterojunctions with enhanced photocatalysis and field emission properties." *J. Appl. Phys.*, **116**, 064305 (2014).
38. H. Li, H. Wu, S. Yuan, and H. Qian, "Synthesis and characterization of vertically standing MoS_2 nanosheets." *Sci. Rep.*, **6**, 21171 (2016).
39. A. V. Agrawal, R. Kumar, S. Venkatesan, A. Zakhidov, Z. Zhu, J. Bao, K. Mahesh, and M. Mukesh, "Fast detection and low power hydrogen sensor using edge-oriented vertically aligned 3-D network of MoS_2 flakes at room temperature." *Appl. Phys. Lett.*, **111**, 093102 (2017).
40. L. Chacko, M. K. Jayaraj, and P. M. Aneesh, "Excitation-wavelength dependent upconverting surfactant free MoS_2 nanoflakes grown by hydrothermal method." *J. Lumin.*, **192**, 6 (2017).
41. A. V. Agrawal, N. Kumar, S. Venkatesan, A. Zakhidov, C. Manspeaker, Z. Zhu, F. R. H. Carlos, J. Bao, and M. Kumar, "Controlled growth of MoS_2 flakes from in-plane to edge-enriched 3-D network and their surface energy studies." *ACS Appl. Nano Mater.*, **1**, 2356 (2018).
42. A. Molina-Sanchez and L. Wirtz, "Phonons in single-layer and few-layer MoS_2 and." *Phys. Rev. B*, **84**, WS2 155413 (2011).
43. S. Chang, T. Hsueh, I. Chen, and B.-R. Huang, "Highly sensitive ZnO nanowire CO sensors with the adsorption of Au nanoparticles." *Nanotechnology*, **19**, 175502 (2008).
44. Z. Li, Y. Huang, S. Zhang, W. Chen, Z. Kuang, D. Ao, W. Liu, and Y. Fu, "A fast response and recovery H_2S gas sensor based on α-Fe_2O_3 nanoparticles with ppb level detection limit." *J. Hazard. Mater.*, **300**, 167 (2015).
45. B. Liu, L. Chen, G. Liu, A. N. Abbas, M. Fathi, and C. Zhou, "High-performance chemical sensing using schottky-contacted chemical vapor deposition grown monolayer MoS_2 transistors." *ACS Nano*, **8**, 5304 (2014).
46. Byungjin Cho et al., "Charge-transfer-based Gas Sensing Using Atomic-layer MoS_2." *Scientific Reports*, **5**, 8052 (2015).
47. D. J. Late et al., "Sensing behavior of atomically thin-layered MoS_2 transistors." *ACS Nano*, **7**, 4879 (2013).
48. Z. Fan and J. G. Lu, "Chemical sensing with ZnO nanowire field-effect transistor." *IEEE Trans. Nanotechnol.*, **5**, 393 (2006).
49. S. Barazzouk, R. P. Tandon, and S. Hotchandani, "MoO_3 - based sensor for NO, NO_2 and CH_4 detection." *Sensors Actuators B*, **119**, 691 (2006).
50. G. A. Asres et al., "Ultrasensitive H_2S gas sensors based on p-type WS_2 hybrid materials." *Nano Res.*, **11**, 4215 (2018).
51. R. Cao, B. Zhou, C. Jia, X. Zhang, and Z. Jiang, "Theoretical study of the NO, NO_2, CO, SO_2, and NH_3 adsorptions on multi-diameter single-wall MoS_2 nanotube." *J. Phys. D: Appl. Phys.*, **49**, 045106 (2016).
52. F. Niu, J. Liu, L. Tao, W. Wang, and W. Song, "Nitrogen and Silica co-doped graphene nanosheets for NO_2 gas sensing." *J. Mater. Chem. A*, **1**, 6130 (2013).
53. G. Lu, L. E. Ocola, and J. Chen, "Reduced graphene oxide for room-temperature gas sensors." *Nanotechnology*, **20**, 445502(1–9) (2009).
54. W. K. Nomani, R. Shishir, M. Qazi, D. Diwan, V. B. Shields, M. G. Spencer, G. S. Tompa, N. M. Sbrockey, and G. Koley, "Chemical highly sensitive and selective detection of NO_2 using epitaxial graphene on 6H-SiC." *Sensors Actuators B*, **150**, 301 (2010).
55. S. Y. Jeong, S. H. Choi, J.-W. Yoon, J. M. Won, Y. C. Kang, J.-S. Park, and J.-H. Lee, "Selective NO_2 sensors using MoS_2-MoO_2 composite yolk-shell spheres." *J. Sens. Sci. Technol.*, **24**, 151 (2015).
56. J. Z. Ou et al., "Physisorption based charge transfer in two-dimensional SnS_2 for selective and reversible NO_2 gas sensing." *ACS Nano*, **9**, 10313 (2015).